



## EFFECT OF RARE EARTH IONS ( $\text{La}^{3+}$ ) ON HUMIDITY SENSING CHARACTERISTICS CADMIUM FERRITES

<sup>1</sup>Gadkari A. B., <sup>2</sup>Shinde T. J. and <sup>3</sup>Vasambekar P. N.

<sup>1</sup>GKG College, Kolhapur (M.S) India

<sup>2</sup>KRP Mahavidyalaya, Isalmpur (M.S) India

<sup>3</sup>Shivaji University, Kolhapur (M.S) India

Email: ashokgadkari88@yahoo.com

**Abstract:** The nanocrystallite powders of La-Cd ferrites were synthesized by oxalate co-precipitation method. The structural analysis was done by XRD, SEM and FT-IR techniques. The X-ray diffraction study shows cubic spinel structure material with crystallite size of range of 28.86 to 30.40 nm. The grain size lies in the range of 0.67 to 1.2  $\mu\text{m}$ . The grain size of  $\text{La}^{3+}$  added cadmium ferrite is smaller than Cadmium ferrite. FT-IR show two absorption band in high and low frequency region. The resistivity of the samples decreases with increase in percentage relative humidity (%RH). The decrease is found to be exponential for 40 to 80 %RH and linear for 80 to 90%RH. The samples are humidity sensitive at low humidity range of 40 to 80%RH. The sensitivity of La-Cd sensor is higher than Cd sensor. The response and recovery time of La-Cd sensor shorter than Cd sensor.

**Keywords:** Synthesis, Crystallite size, Humidity, Response time

### Introduction:

An accurate control, monitoring of water content estimate are practically essential in various fields, including air quality detection, inflammable gas inspection, food, healthcare, clinical, biological sectors and defense [1]. Many scientific and technological efforts have been made for humidity sensors, to improve their selectivity, stability and response/recovery for particular use [2]. The research laboratory and clean room environment is highly affected by moisture levels and require constant monitoring. Recently monitoring and auto-controlling of local humidity environment has become important topic in the field of industry, agriculture, military and house hold [3].

The humidity sensors are required with a small size and high sensing resolution [4]. The porous material can be used as humidity sensors [5-10]. The conductance-humidity sensitivity of the ceramic sensors is determined by the material itself, the sintering conditions, and the preparation method. Some polycrystalline ferrites can be used as good humidity sensor elements. The porosity of ferrites is advantageous when they are used as humidity sensors. They can give the change in resistivity of about three orders of magnitude with changes in the surrounding humidity [11].

In this paper, we report effect of  $\text{La}^{3+}$  ions addition on humidity sensing properties of Cd ferrites.

### Materials and Method:

#### Synthesis and Characterization

Polycrystalline powders 5 wt% rare earth elements  $\text{La}^{3+}$  added  $\text{CdFe}_2\text{O}_4$  samples were prepared by the oxalate co-precipitation method using sulphates. The detail method of synthesis for sample under investigation is reported elsewhere [12]. The polycrystalline ferrite powder under investigation, were characterized by X-ray powder diffraction on Philips PW-3710 X-ray diffractometer with  $\text{CuK}_\alpha$  radiation ( $\lambda = 1.5424 \text{ \AA}$ ). Each sample was scanned in range  $20^\circ$  to  $80^\circ$  with a step size of  $0.02^\circ$ . The X-ray tube was excited at 40 kV and 0.03 A. The SEM micrographs of fractured were recorded on scanning electron microscope, JEOL – JSM 6360 model, Japan. The FT-IR absorption spectra of powered samples were recorded in the range  $350 \text{ cm}^{-1}$  –  $800 \text{ cm}^{-1}$ , on a Perkin-Elmer model: Spectrum one FT-IR spectrometer by KBr pellet technique.

#### Humidity Sensing Characteristic

The humidity testing of samples was conducted in a microprocessor controlled humidity chamber (Aditi Associate make, Model ASC-10, Mumbai) in the range of 40%RH to 90%RH in steps of 10%RH. The

sensor elements (pellets) about 2mm thickness and 13mm diameter were fixed in conducting cell. For good electrical contact silver contacts were made on sensor element. DC voltage was applied across the sensor element with the help of constant potential voltage source. The resistance of sensor (pellet) was measured by two probe method with a picometer. The measurement was performed at the temperature 27°C.

## Results and Discussion:

### Characterization

The structural characterization (XRD, SEM and FT-IR) of 5 wt% La<sup>3+</sup> added Cd ferrites under investigations is already reported [13]. The typical XRD patterns of 5 wt% La<sup>3+</sup> added CdFe<sub>2</sub>O<sub>4</sub> confirms the formation of cubic spinel with orthoferrite secondary phase (Fig. 1). The average crystallite size of the samples is in the range of 28.86 to 30.40 nm.

The lattice constant, crystallite size and grain size of all the samples under investigation is listed in table I. From this table, it is observed that lattice constant of prepared by oxalate co-precipitation method are very close to those reported for samples prepared by ceramic method [14]. Such reduction in the lattice constant in rare-earth ions substituted ferrites has been reported by E. Rezlescu and N. Rezlescu [15], suggesting the occupancy of rare earth ion on B-sites. Similar results for rare-earth element added ferrites have been reported [13-15].

The porosity of all the samples are given in Table I shows that X-ray density ( $\rho_x$ ) is higher than physical density. This is attributed to formation of these secondary phase which favors the inhabitation of grain growth [13].

The microphotographs of 5wt% La<sup>3+</sup> ions added CdFe<sub>2</sub>O<sub>4</sub> is presented in Fig. 2. The average grain size lies in the range of 0.67  $\mu$ m to 1.2  $\mu$ m. The grain size decreases with addition of rare earth elements in Cd ferrites [14].

Typical Infrared absorption spectra of 5 wt% La<sup>3+</sup> added CdFe<sub>2</sub>O<sub>4</sub> is presented in Fig. 3. The high and low frequency absorption bands ( $\nu_1$ ,  $\nu_2$ ) are observed in frequency

range 555.27 to 468.12 cm<sup>-1</sup> and 554.76 to 469.60 cm<sup>-1</sup> respectively. These bands are common characteristics of spinel ferrites [16].

### Humidity sensing

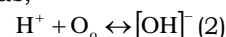
Variation of resistivity with humidity (% RH) of ferrite sensors is presented in Fig. 4. All the samples exhibit a significant decrease in the electrical resistivity with increased relative humidity in the range of 40 to 90 %RH. The resistivity of these sensor elements follows the equation [15],

$$\rho = \rho_0 e^{-SRH} \quad (1)$$

where, S - humidity sensitivity and RH - relative humidity.

The humidity is surface adsorption phenomenon in which higher humidity sensitivity is attributed to higher surface area of the samples. At low humidity, water adsorption on surface is dominant factor for electrical conductance. The higher surface area would provide more sites for water adsorption and produce more charge carriers for electrical conductance [17].

The fall in resistivity between 40 to 90 %RH for all the samples is due to increase in electrical conductance or charge carriers. All the samples show decrease in resistivity with increase in %RH indicating the conductance occurs at the grain surface is due to water adsorption of molecule. At low humidity levels chemisorption takes place leading to formation of two hydroxyl group with charge transports occurring by hopping mechanism [19]. At higher %RH physisorption of water molecules and electrolytic conduction takes place. The adsorption of humidity on the surface decreases the resistivity due to the increase of charge carriers, protons, in the ferrite and water system [18]. The adsorption of water on the surface of the material leads to the dissociation of hydrogen ions. These hydrogen ions bonded with the surface lattice oxygen atom, forms the hydroxyl groups [20] as,



Where, O<sub>o</sub> - corresponds to oxygen at lattice sites. These hydroxyl groups are bonded with the lattice iron atoms and liberate the

free electrons [9] giving increase in conductivity as,



Thus the conductivity increases with increased humidity [18, 19].

It is seen from table that, the sensitivity of all the samples increases with increase in radius of rare earth ions which is attributed to increase in porosity. Kotnala *et al.* [21] reported increase in sensitivity for lithium substituted magnesium ferrite in the range 10-80%RH. All the samples are humidity sensitive in lower humidity range.

The large decrease in resistivity with increased % RH is related to adsorption of water molecules on the surface and condensation in capillary pores. These samples have smaller grain size. This smaller grains leads to much more grain boundaries and thus to more active sites available for water adsorption. The decreased resistivity at higher %RH of the samples is due to lesser porosity of the samples. At higher %RH the adsorbed water molecules condense in capillary pores, resulting electrolytic conductance. Rezlescu *et al* [15] reported compositional dependence of humidity sensitivity of Ga and La substituted Mg-Cu ferrites.

The response/recovery time of all samples lies between 160-285 s. The Sm-Cd ferrite sensor is having shortest response time. The sensors show shorter response time than Cd ferrite sensors [22]. This is because of the decrement in the grain size due to formation of secondary phase on grain boundaries of these sensors and highest of porosity in this sensor. The recovery time of these sensors is also smaller than that of Cd ferrite sensors.

### Conclusion:

The nanocrystallite powders of Sm-Cd ferrites were prepared by oxalate co-precipitation method. The XRD confirms the formation of cubic spinel with orthoferrite secondary phase. The average crystallite size of the samples is in the range of 28.86 to 30.40 nm. The grain size obtained from SEM study is in the range of 0.67 to 1.2  $\mu\text{m}$ . The grain size of  $\text{Sm}^{3+}$  added cadmium ferrite is smaller than cadmium ferrite. FT-IR show two absorption band in high and low frequency region. All the samples are humidity sensitive at low humidity range of 40 to 80%RH. The sensitivity of La-Cd sensor is higher than Cd sensor. The response and recovery time of La-Cd sensor shorter than Cd sensor.

Table-1. Parameters of 5 wt% rare earth element ( $\text{La}^{3+}$ ) added  $\text{CdFe}_2\text{O}_4$

Rare earth ion	Crystallite Size D (nm)	Lattice Constant a ( $\text{\AA}$ )	Grain Size ( $\mu\text{m}$ )	X-ray Density $\rho_x$ (gm/cc)	Physical Density $\rho_p$ (gm/cc)	Porosity P (%)	Humidity Sensitivity ( $\text{M}\Omega/\text{\%RH}$ )	Response and Recovery time (sec)	
								Res	Reco
Cd	30.40	8.71	1.2	5.78	4.74	17.99	58.03	170	285
$\text{Sm}^{3+}$	28.86	8.69	0.67	6.12	4.95	19.07	5839.66	110	140

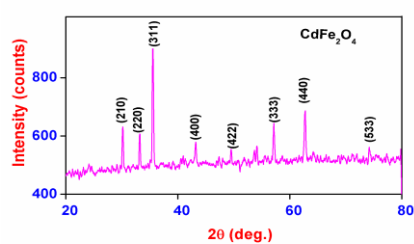


Fig. 1: Typical X-ray diffraction patterns of  $\text{CdFe}_2\text{O}_4$

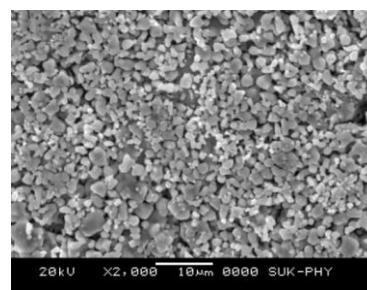


Fig. 2: SEM micrograph of 5 wt%  $\text{La}^{3+}$  ions added  $\text{CdFe}_2\text{O}_4$

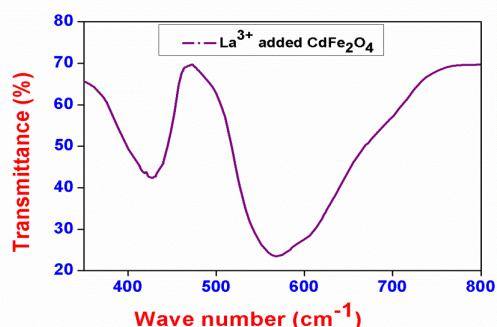


Fig. 3: Typical FT-IR spectra of 5 wt% La<sup>3+</sup> ions added CdFe<sub>2</sub>O<sub>4</sub>

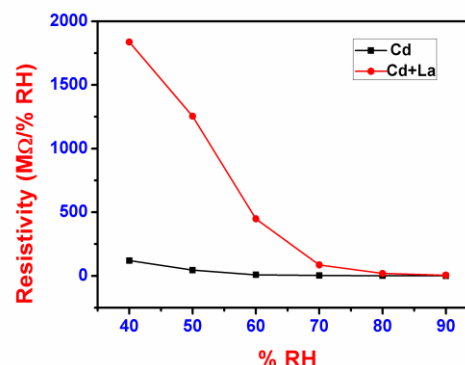


Fig. 4: Variation of resistivity ( $\rho$ ) – (%RH) characteristics for La– Cd ferrite

#### References:

- B. Ostrick, R. Pohle, M. Fleischer and H. Heixner**, *Sensors and Actuators B:Chem.*, 68(1-3), (2000), pp. 234-239.
- Y. Feng, S. Wang, B. Feng, Y. He and T. Zhang**, *Sensors and Actuators A*, 152, (2009), pp. 104-109.
- L. Hongxia, S. Zhiming, L. Hongwei, J. Rare Earths**, 28(1), (2010), pp.123-127.
- J T W Yeow and J P M She**, *Nanotechnology*, 17(21), (2006), pp. 5441-5448.
- A. B. Gadkari, T J Shinde & P. N. Vasambekar**, *International J. of Research in Bioscience, Agriculture & Technology*, 29(7), (2015), pp.214-216.
- F. M. Faia, C. S. Furtado and A. J. Ferrira**, *Sensors and Actuators B:Chem.*, 107(2), (2005), pp. 353-359.
- K. Arshaka, K. Twomej and D. Egan**, *Sensors*, 2(2), (2002), pp. 50-61.
- N. Begum, M. A. Gafur, A. H. Bhuiyan and D. K. Saha**, *Phys. Status Solidi A*, 207(4), 2010, pp. 986-992.
- H. Arai, S. Ezaki, Y. Shimizu , O. Shippo and T. Seiyama**, *Proceedings International Meeting on Chemical Sensors*, 1983, pp.393.
- J. H. Anderson and G. A. Parks**, *J. Phys. Chem.*, 72, (1968), pp. 3362-3368,
- C. Dorofiti, E. Rezlescu, N. Rezlescu, P. D. Popa**, *Sensors and Actuators*, 115(20), (2006), pp. 589-596,
- ABG, T J Shinde & P. N. Vasambekar**, *Rare Metal*, 29(2), (2016), PP. 168-173.
- A. B. Gadkari, T J Shinde & P. N. Vasambekar**, *Journal of Alloys and Compounds*, 509(3), (2011), pp. 966-972.
- JL Bhosale, E. Relescu, N Relescu & P D popa** *Physics stat. Sol (c)*, (12), (2004), PP 3636-3639.

- R. D. Waldron**, *Phy-Rev*, 99(6), (1955), PP. 1727-1735.
- K. S. Chou, T. K. Lee, F. J. Liu**, *Sens. Actuators B: Chem.*, 56(1-2), (1999), pp. 106-111.
- R. Sundaram, E. S. Raj and K. S. Nagaraja**, *Sens. Actuators B: Chem.*, 99(2-3), (2004), pp. 350-354.
- R. Sundaram and K. S. Nagaraja**, *Sens. Actuators B: Chem.*, 101(3), (2004), pp. 353-360.
- X. Q. Liu, S. W. Tao and Y. S. Shen**, *Sens. Actuators B: Chem.*, 40(1-2), (1997), pp. 161-165.
- R. K. Kotnala, J. Shah, B. Sing, H. Kishan, S. Sing, S. K. Dhawan, A. Sengupta**, *Sensors and Actuators B: Chem.*, 29(2), (2008), pp.909-914.
- A. B. Gadkari, T. J. Shinde and P. N. Vasambekar**, *Adv. Mater. Res.*, 645, (2013), pp. 160-163,

\*\*\*\*\*